

FUSE: Label-Free Image-Event Joint Monocular Depth Estimation via Frequency-Decoupled Alignment and Degradation-Robust Fusion

Pihai Sun¹, Junjun Jiang^{1*}, Yuanqi Yao¹, Youyu Chen¹, Wenbo Zhao¹, Kui Jiang¹, Xianming Liu¹

Abstract—Image-event joint depth estimation methods leverage complementary modalities for robust perception, yet face challenges in generalizability stemming from two factors: 1) limited annotated image-event-depth datasets causing insufficient cross-modal supervision, and 2) inherent frequency mismatches between static images and dynamic event streams with distinct spatiotemporal patterns, leading to ineffective feature fusion. To address this dual challenge, we propose Frequency-decoupled Unified Self-supervised Encoder (*FUSE*) with two synergistic components: The Parameter-efficient Self-supervised Transfer (PST) establishes cross-modal knowledge transfer through latent space alignment with image foundation models, effectively mitigating data scarcity by enabling joint encoding without depth ground truth. Complementing this, we propose the Frequency-Decoupled Fusion module (FreDFuse) to explicitly decouple high-frequency edge features from low-frequency structural components, resolving modality-specific frequency mismatches through physics-aware fusion. This combined approach enables *FUSE* to construct a universal image-event encoder that only requires lightweight decoder adaptation for target datasets. Extensive experiments demonstrate state-of-the-art performance with 14% and 24.9% improvements in Abs.Rel on MVSEC and DENSE datasets. The framework exhibits remarkable zero-shot adaptability to challenging scenarios including extreme lighting and motion blur, significantly advancing real-world deployment capabilities. The source code for our method is publicly available at: <https://github.com/sunpihai-up/FUSE>.

I. INTRODUCTION

Modern monocular depth estimation (MDE) increasingly utilizes multi-modal sensing to address the limitations of single-sensor systems [6, 27], particularly by integrating conventional image sensors with emerging event cameras. Traditional image sensors, which operate using fixed-exposure light integration, effectively preserve structural information but suppress high-frequency temporal variations. This characteristic makes them suitable for static scene perception but limits their performance in dynamic scenarios. In contrast, event cameras asynchronously detect pixel-wise brightness changes with microsecond resolution [35], making them highly effective for capturing high-frequency motion but incapable of detecting static structures with subthreshold intensity gradients. The inherent complementarity in the frequency domain between these two modalities highlights the potential of image-event fusion as a promising approach for achieving robust depth estimation in dynamic environments.

Recent studies [6, 17, 14] have explored leveraging the complementary characteristics of image and event modalities

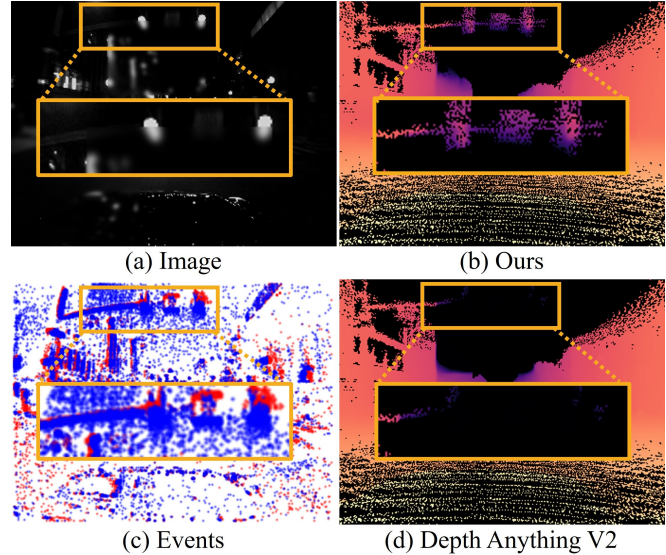


Fig. 1. **Demonstration of *FUSE*'s superior performance in challenging conditions.** (a) and (c) show the input image and event data, with blue/red in (c) indicating brightness decrease/increase. When image data fails due to low light and blur, event data provides complementary dynamic information. Our method (d) leverages multimodal synergy, recovering the traffic light missed by the state-of-the-art image depth model [28], as highlighted in the orange box.

for joint MDE. These methods typically encode both modalities into a unified feature space, followed by customized feature fusion modules for depth prediction. However, their reliance on supervised learning with depth ground truth from image-event pairs has revealed poor generalization capabilities. This limitation arises from the scarcity and limited diversity of existing labeled image-event datasets [36] compared to large-scale image-depth datasets such as NYUv2 [25] and KITTI [8].

Additionally, although the frequency-domain complementarity between images and events presents theoretical advantages, mismatches in their frequency characteristics introduce significant challenges for feature fusion. Conventional fusion strategies risk destructive interference [2]: high-frequency event features can disrupt the structural continuity of image representations, while low-frequency image components may suppress critical motion cues captured by events. This inherent frequency divergence, combined with limited training data, poses a dual challenge—requiring models to bridge the modality gap with insufficient supervision and resolve conflicting frequency signatures during feature integration.

Inspired by the impressive generalization capabilities of image-based depth foundation models (e.g., Depth Anything [29]), which are trained on millions of images, we

¹Faculty of Computing, Harbin Institute of Technology

*Corresponding author

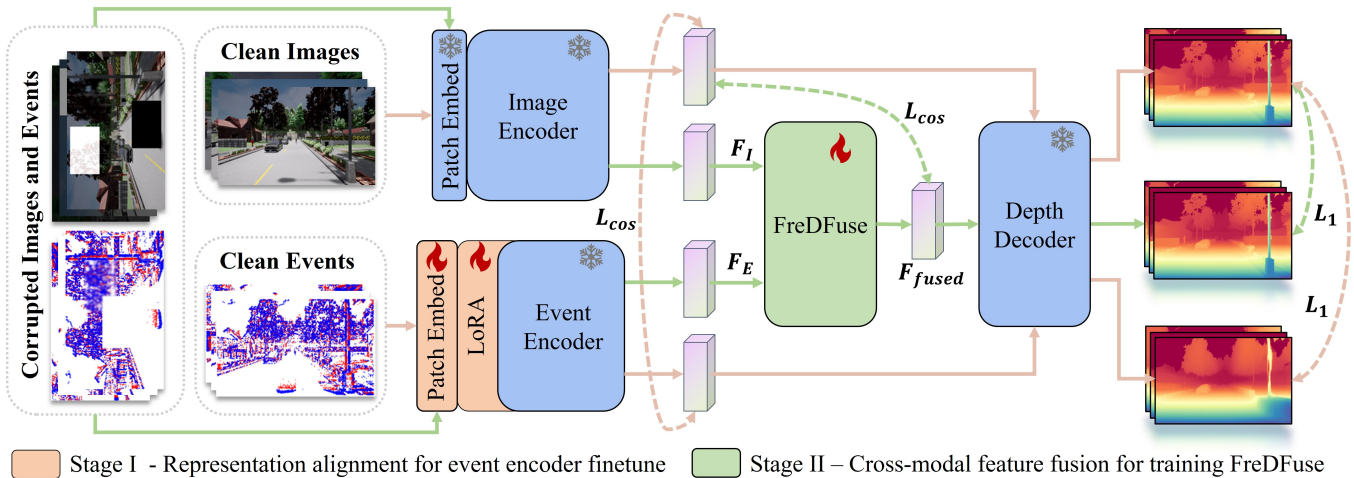


Fig. 2. **Overview of the FUSE framework.** FUSE integrates an image encoder, event encoder, Frequency-Decoupled Fusion module (FreDFuse), and depth decoder. The image encoder and depth decoder are initialized with a pre-trained MDE model. A two-stage knowledge transfer strategy fine-tunes the event encoder and FreDFuse. In Stage I, the event encoder is initialized with the image encoder’s weights, and only the LoRA matrix and Patch Embed are fine-tuned using clean event data. In Stage 2, randomly degraded image-event pairs are used, and only the FreDFuse is fine-tuned. The MDE model supervises both stages with clean image data in the output and latent spaces.

propose a potential solution: transferring their well-learned image-depth priors to bridge the gap between event-based and depth-based representations. This insight motivates our two-fold innovation: 1) addressing data scarcity through parameter-efficient transfer learning, and 2) resolving intrinsic frequency mismatches via frequency decoupling mechanisms.

We introduce FUSE, a frequency-decoupled, unified, self-supervised encoder-based method designed to transfer knowledge from image-based depth models to image-event joint (MDE) without requiring depth ground truth. FUSE consists of two main components: 1) Parameter-Efficient Self-Supervised Transfer (PST): A two-phase training strategy with decoupled feature alignment and fusion stages. In Phase I, an event encoder is trained using lightweight adapter tuning to establish a shared latent space between image and event modalities. Phase II focuses on frequency-aware fusion training, incorporating a novel fusion module, FreDFuse, under simulated sensor degradation conditions; 2) Frequency-Decoupled Fusion Module (FreDFuse): Serving as the core of PST’s second phase, this module separates features into distinct frequency components before fusion. By utilizing frequency-specific processing pipelines, it enables complementary integration while minimizing inter-frequency interference, thus overcoming the limitations of traditional single-bandwidth fusion approaches.

To validate the effectiveness of FUSE, we conduct extensive experiments on the MVSEC and DENSE datasets, demonstrating state-of-the-art (SOTA) performance in MDE. As shown in Fig. 1, FUSE outperforms the current SOTA image depth model [28] under zero-shot settings, particularly in night-time driving scenarios affected by motion blur, highlighting its robustness. In summary, our contributions are as follows:

- We propose FUSE, the first self-supervised framework

for generalizable image-event depth estimation that transfers knowledge from image-only depth foundation models without requiring depth-labeled image-event pairs. This addresses the critical challenge of scarce annotated image-event-depth datasets.

- Parameter-Efficient Self-Supervised Transfer (PST): A novel two-stage training strategy that bridges the image-event representation gap through lightweight LoRA-based tuning and degradation-robust distillation, significantly reducing trainable parameters compared to full fine-tuning.
- Frequency-Decoupled Fusion Module (FreDFuse): A frequency-aware fusion module that explicitly disentangles high-frequency edge dynamics (from events) and low-frequency structural priors (from images). This approach resolves modality-specific frequency mismatches while preserving complementary cues.

II. RELATED WORK

A. Image-based Monocular Depth Estimation

Deep learning-based methods have become the dominant paradigm in MDE. Eigen et al. [4] were the first to introduce a multi-scale fusion network for depth prediction through regression. Subsequent studies have improved depth estimation accuracy by reformulating the regression task as classification [1, 13, 21], introducing novel network architectures [18], and incorporating additional prior knowledge [22, 31]. Despite these advancements, the generalization capability of such models remains a major challenge. To address this limitation, recent research [19, 30] has focused on training models on large-scale datasets aggregated from diverse sources, leading to substantial improvements. A milestone in this direction is MiDaS [19], which mitigates the impact of varying depth scales across datasets by employing an affine-invariant loss. More recently, the DepthAnything series [29,

28] has further enhanced the utilization of unlabeled data alongside large-scale labeled datasets, achieving remarkable performance. However, due to the inherent limitations of traditional image cameras, image-based MDE methods are still susceptible to factors such as lighting conditions and motion blur, which can degrade their performance [3, 26, 12].

B. Event-based Monocular Depth Estimation

Event-based MDE methods have attracted attention for their effectiveness under extreme lighting and high-speed motion conditions, making them suitable for applications in autonomous driving and robotic navigation [5]. E2Depth [10] was the first method to propose dense MDE using event data, employing a recurrent encoder-decoder architecture. Mixed-EF2DNet [23] introduced a flow network to capture temporal information effectively, while EReFormer [15] leveraged a Transformer-based architecture for improved performance. Additionally, HMNet [9] incorporated multi-level memory units to handle long-term dependencies efficiently. Nonetheless, these methods continue to face challenges due to the sparsity of event data and the limited availability of training datasets [20].

C. Image-Event Fusion

The complementary characteristics of event and image data have been leveraged to enhance various visual tasks, including semantic segmentation [32, 32], object detection [33, 34], and depth estimation [6, 17]. RAMNet [6] employs an RNN-based approach to effectively utilize asynchronous event data, while EVEN [24] improves low-light performance by fusing modalities prior to inputting them into an MDE network. SRFNet [17] guides modality interaction using spatial reliability masks, and PCDepth [14] integrates features at the modality level for more effective fusion. Our *FUSE* is the first to leverage knowledge transfer from an image foundation model for both feature encoding and fusion, significantly enhancing robustness and accuracy in image-event joint depth estimation.

III. METHODOLOGY

A. Overview

In this section, we introduce *FUSE*, a low-cost and robust transfer learning framework for generalizable depth prediction. An overview of the *FUSE* architecture is provided in Fig. 2, our framework consists of four key components: an event encoder \mathcal{E}_E , an image encoder \mathcal{E}_I , a Frequency-Decoupled Fusion module (FreDFuse), and a depth decoder \mathcal{D} . Given an input image \mathbf{I} and its event stream \mathbf{S} , the target is to predict the dense depth map \mathbf{d}^* . Our *FUSE* provides a powerful image-event joint encoder (\mathcal{E}_I , \mathcal{E}_E , FreDFuse) with exceptional generalization capabilities, enabling robust performance with minimal adaptation of the depth decoder for target datasets.

In Sec.III-B, we first describe the event processing pipeline. Subsequently, in Sec.III-C, we detail the process of obtaining the image-event joint encoder via PST. Finally, in Sec. III-D, we present the FreDFuse in detail.

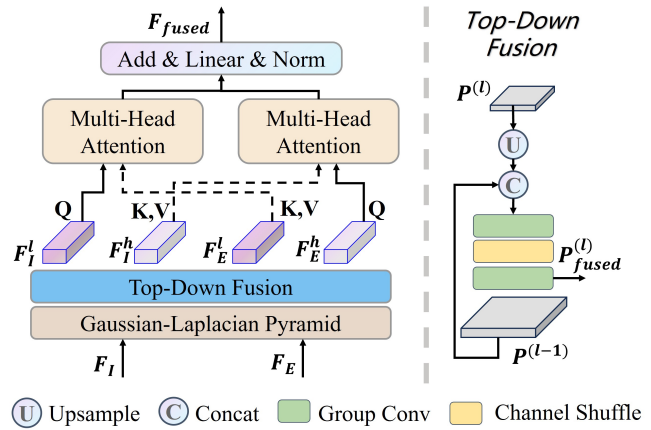


Fig. 3. **Overview of our FreDFuse.** FreDFuse decouples image features F_I and event features F_E into high- and low-frequency components using a Gaussian-Laplacian pyramid. Multi-scale features are fused top-down with 1×1 group convolutions and channel shuffle. Fusion in the high-frequency branch is event-driven, while the low-frequency branch is image-driven. The high- and low-frequency components are combined through addition and processed by LayerNorm.

B. Event Representation

The event stream is first transformed into a voxel grid representation [6] to make it compatible with existing network architectures. Each event e_n is represented by the tuple (x_n, y_n, t_n, p_n) , which means that at time t_n , the log intensity change at the pixel position (x_n, y_n) exceeds a threshold. The polarity p_n (± 1) indicates whether the intensity increases or decreases. As such, the asynchronous event stream $\mathbf{S} = \{e_n\}_{n=0}^{N-1}$ must be transformed into a frame-like representation to be compatible with existing network architectures. Following prior works [6], [17], [14], [10] we convert the temporal stream of events into a voxel grid [7].

Given an event stream $S = \{e_n\}_{n=0}^{N-1}$ within the time interval $\Delta T = t_{N-1} - t_0$, we transform it into a voxel grid with spatial dimensions $H \times W$ and B time bins:

$$V(x, y, t) = \sum p_i \delta(x - x_i, y - y_i) \max\{0, 1 - |t - t_i^*|\} \quad (1)$$

where $t_i^* = \frac{B-1}{\Delta T}(t_i - t_0)$. The voxel grid $V \in \mathbb{R}^{H \times W \times B}$. We choose $B = 3$ time bins.

The similar structural form facilitates knowledge transfer from image-based models, enabling the leveraging of pre-trained networks for enhanced performance. At the same time, the image data can be used without additional processing.

C. Parameter-efficient Self-supervised Transfer

Our Parameter-efficient Self-supervised Transfer (PST) strategy addresses the critical challenge of event-based depth estimation data scarcity by establishing a unified foundation model for image-event joint MDE through efficient cross-modal knowledge transfer. This self-supervised approach eliminates dependency on expensive depth ground truth while achieving two key objectives: 1) transferring image domain priors to the image-event joint domain using only paired image-event data, and 2) preserving the foundation model's generalization capability through parameter-efficient

TABLE I

QUANTITATIVE RESULTS ON THE MVSEC DATASET [36]. \downarrow INDICATES LOWER IS BETTER AND DENOTES HIGHER IS BETTER. THE BEST RESULTS ARE HIGHLIGHTED IN BOLD, WHILE THE SECOND-BEST OUTCOMES ARE UNDERLINED.

Methods	Input	outdoor day1						outdoor night1					
		$\delta_1 \uparrow$	$\delta_2 \uparrow$	$\delta_3 \uparrow$	Abs.Rel \downarrow	RMSE \downarrow	RMSELog \downarrow	$\delta_1 \uparrow$	$\delta_2 \uparrow$	$\delta_3 \uparrow$	Abs.Rel \downarrow	RMSE \downarrow	RMSELog \downarrow
E2Depth[10]	E	0.567	0.772	0.876	0.346	8.564	0.421	0.408	0.615	0.754	0.591	11.210	0.646
EReFormer[15]	E	0.664	0.831	0.923	0.271	-	0.333	0.547	0.753	0.881	0.317	-	0.415
HMNet[9]	E	0.690	0.849	0.930	0.254	6.890	0.319	0.513	0.714	0.837	0.323	9.008	0.482
RAMNet[6]	I+E	0.541	0.778	0.877	0.303	8.526	0.424	0.296	0.502	0.635	0.583	13.340	0.830
SRFNet[17]	I+E	0.637	0.810	0.900	0.268	8.453	0.375	0.433	0.662	0.800	0.371	11.469	0.521
HMNet[9]	I+E	<u>0.717</u>	<u>0.868</u>	0.940	0.230	6.922	0.310	0.497	0.661	0.784	0.349	10.818	0.543
PCDepth[14]	I+E	0.712	0.867	<u>0.941</u>	<u>0.228</u>	<u>6.526</u>	<u>0.301</u>	0.632	<u>0.822</u>	<u>0.922</u>	<u>0.271</u>	<u>6.715</u>	<u>0.354</u>
FUSE (Ours)	I+E	0.745	0.892	0.957	0.196	6.004	0.270	<u>0.629</u>	0.824	0.923	0.261	6.587	0.351

adaptation. As shown in Fig. 2, PST operates through two cascaded stages:

Stage I: Parameter-Efficient Feature Alignment: In this stage, we align event data representations with the image domain’s latent space. We initialize \mathcal{E}_E and \mathcal{D}_E using weights from Depth Anything V2 [28] to inherit its geometric understanding ability. To enable efficient adaptation while preventing catastrophic forgetting [16], we implement LoRA[11], where only the LoRA matrices and PatchEmbed Layer parameters (1.8% of \mathcal{E}_E) are updated. This allows adaptation to event data while retaining the foundation model’s generalization capability. The alignment is driven by a compound objective function (detailed in Sec. III-E) that enforces consistency in both output space (depth prediction) and latent representations.

Stage II: Robust Feature Fusion: In this stage, we focus on training the FreDFuse (Sec. III-D) in the image-event joint estimator to robustly fuse multi-modal features from image and event. The image encoder \mathcal{E}_I and decoder \mathcal{D} are inherited from the image foundation model, e.g., Depth Anything V2, while the event encoder \mathcal{E}_E is obtained from Stage I. Only the FreDFuse is trainable during this stage. To improve the robustness and generalization of the proposed method, we also generate randomly degraded image-event pairs as inputs during training. The degraded inputs incorporate diverse noise types, including brightness adjustment, overexposure, motion blur, and occlusion masking. This systematic degradation strategy compels the feature fusion module to identify robust cross-modal relationships that withstand various sensor-specific degradations, thereby enhancing the model’s generalizability and resilience. Here, we use the same objective as Eq. 10 to maintain cross-modal consistency.

D. Frequency-Decoupled Fusion Module

To leverage the complementary characteristics of different visual sensors, we propose a frequency-decoupled fusion method. Image sensors excel at capturing low-frequency static scenes, while event cameras are adept at detecting high-frequency dynamic changes. Our Frequency-Decoupled Feature Integration module (FreDFuse) leverages these complementary strengths by processing and fusing features in separate frequency domains, enabling more effective multi-

modal depth estimation. Fig. 3 shows the overview of FreD-Fuse.

Frequency Decoupling via Gaussian-Laplacian Pyramids: Given token sequences from image features $\mathbf{F}_I \in \mathbb{R}^{B \times N \times C}$ and event features $\mathbf{F}_E \in \mathbb{R}^{B \times N \times C}$, we first decompose them into low-frequency and high-frequency components using Gaussian-Laplacian pyramids. For each modality $m \in \{I, E\}$, the decomposition is formulated as:

$$\mathbf{G}_m, \mathbf{L}_m = \mathcal{P}_m(\mathbf{F}_m), \quad (2)$$

where $\mathcal{P}_m(\cdot)$ denotes the Gaussian-Laplacian decoupling operator. Specifically, the input tokens are reshaped into 2D feature maps and processed through multi-scale pyramids. The Gaussian pyramid \mathbf{G}_m captures low-frequency components via iterative blurring and downsampling:

$$\mathbf{G}_m^{(l)} = \text{Down}(\text{GaussianBlur}(\mathbf{G}_m^{(l-1)})), \quad (3)$$

where $l \in \{1, \dots, L\}$, $L = 3$ denotes the pyramid level. The Laplacian pyramid \mathbf{L}_m , encoding high-frequency details, is derived by subtracting upsampled Gaussian levels:

$$\mathbf{L}_m^{(l)} = \mathbf{G}_m^{(l)} - \text{Up}(\mathbf{G}_m^{(l+1)}). \quad (4)$$

Top-Down Fusion of Multi-Level Pyramid Features: For each pyramid $(\mathbf{G}_I, \mathbf{L}_I, \mathbf{G}_E, \mathbf{L}_E)$, multi-scale features are fused by upsampling and concatenating layers, followed by grouped convolutions:

$$\mathbf{P}_{\text{cat}}^{(l)} = \text{Concat}(\mathbf{P}^{(l-1)}, \text{Up}(\mathbf{P}^{(l)})), \quad (5)$$

$$\mathbf{P}_{\text{comp}}^{(l)} = \text{GroupConv}_{1 \times 1}(\mathbf{P}_{\text{cat}}^{(l)}), \quad (6)$$

$$\mathbf{P}_{\text{fused}}^{(l)} = \text{GroupConv}_{1 \times 1}(\text{ChannelShuffle}(\mathbf{F}_{\text{comp}}^{(l)})). \quad (7)$$

Cross-Branch Frequency-Guided Fusion: The decoupled features are fused in two branches, each guided by the dominant modality in the target frequency band. For the high-frequency branch, $\mathbf{F}_E^{\text{high}}$ is the Query, while $\mathbf{F}_I^{\text{high}}$ is the Key and Value. For the low-frequency branch, $\mathbf{F}_I^{\text{low}}$ is the Query, while $\mathbf{F}_E^{\text{low}}$ is the Key and Value. Both branches use multi-head cross-attention:

$$\text{Attn}(\mathbf{Q}, \mathbf{K}, \mathbf{V}) = \text{Softmax}\left(\frac{\mathbf{Q}\mathbf{K}^T}{\sqrt{d}}\right)\mathbf{V}, \quad (8)$$

where d is the dimension of each attention head. The fused features are recombined and projected to the original space:

$$\mathbf{F}_{\text{fused}} = \text{LayerNorm}(\text{Linear}(\mathbf{F}_{\text{low}} + \mathbf{F}_{\text{high}})). \quad (9)$$

E. Optimization Objectives

Optimization Objective of PST: The PST framework adopts a compound loss to achieve two critical objectives: 1) prediction-level distillation via output-space alignment, and 2) latent-space regularization to preserve transferable representations. Given clean image \mathbf{I} , the image foundation model generates pseudo depth \mathbf{d} and latent features \mathbf{F} , which provide supervision for Stage I and Stage II. The depth map and latent features of the output of Stage I and Stage II are defined as \mathbf{d}^* and \mathbf{F}^* . We formulate a compound loss function L_{align} :

$$L_{\text{align}} = L_1 + L_{\text{cos}}, \quad (10)$$

where $L_1 = \|\mathbf{d} - \mathbf{d}^*\|_1$ aligns output predictions, and $L_{\text{cos}} = [1 - \cos(\mathbf{F}, \mathbf{F}^*)] \cdot \mathbb{I}(\alpha \leq \cos(\mathbf{F}, \mathbf{F}^*) \leq \beta)$ aligns latent representations. Here, $\alpha = 0.2$, $\beta = 0.85$, and $\mathbb{I}(\cdot)$ ensure loss activation within the specified similarity range, preventing over-regularization.

Optimization Objective of Target Datasets: When transferring to target datasets with metric depth labels, we replace pseudo-supervision with the Scale-invariant Logarithmic (SiLog) loss [4]. Given a predicted depth map \mathbf{d}^* and depth ground truth \mathbf{d} , the loss is computed over the pixels as follows:

$$L_{\text{SiLog}} = \sqrt{\frac{1}{N} \sum_i e_i^2 - \lambda \left(\frac{1}{N} \sum_i e_i \right)^2}, \quad (11)$$

where $e_i = \ln d_i - \ln d_i^*$, N is the total number of valid pixels.

IV. EXPERIMENT

To validate the effectiveness of our proposed *FUSE* framework in addressing the scarcity of event-depth data and modality disparity, we conduct comprehensive experiments under strictly controlled conditions. Our evaluation protocol emphasizes three critical aspects: (1) Generalization capability across real-world (MVSEC) and synthetic (DENSE) scenarios; (2) Performance constraints with frozen image-event joint encoders; (3) Computational efficiency in multi-modal fusion.

A. Experimental Settings

We utilize EventScape [6] for image-event pairs in PST (without depth ground truth). We evaluate on MVSEC [36] and DENSE [10] datasets, where MVSEC is a real-world scenario while EventScape and DENSE are synthetic scenarios.

MVSEC Dataset: The MVSEC dataset uses a pair of DAVIS cameras to capture grayscale images and event data at a resolution of 346×260 . Depth ground truth is recorded using a LiDAR sensor at 20 Hz. Grayscale images are captured at 10 Hz during the day and 45 Hz at night.

Metrics: Following [14], we evaluate performance using the metrics: Absolute Relative Error (Abs.Rel), Root Mean

Square Error (RMSE), Logarithmic Squared Error (RMSELog), average absolute depth errors at different cut-off depth distances (i.e., 10m, 20m, and 30m), and accuracy ($\delta < 1.25^n$, $n = 1, 2, 3$).

Implementation Details: The model is trained using the Adam optimizer with a learning rate of $5e-5$, implemented in PyTorch on two RTX 3090ti GPUs with a batch size of 48. PST on EventScape [6] is trained for 10 epochs, and fine-tuning on MVSEC and DENSE for 20 epochs. Manual alignment is needed for the MVSEC dataset due to the asynchronous nature of images, events, and depth labels. As in [14], event data from the first 50 ms prior to each depth ground truth is paired with the most recent image to form the data pairs.

B. Evaluation on MVSEC and DENSE Datasets

We report quantitative results on the real-world MVSEC [36] and synthetic DENSE [10] datasets. For MVSEC, we use the outdoor_day2, outdoor_night2, and outdoor_night3 sequences for training, and outdoor_day1 and outdoor_night1 for testing, with depth range from 1.97 to 80 meters [14]. For DENSE, we use the provided training and test sets, with depth range from 3.34 to 1000 meters [6, 17]. We freeze the image-event joint encoder and train only the depth decoder.

Analysis on MVSEC Dataset: Tab. I presents a quantitative comparison between our method and SOTA methods for event-based estimation and image-event joint estimation on the MVSEC dataset. In the outdoor_day1 scene, our method outperforms the best image-event joint estimation approach [14] by 14% and 10.2% in Abs.Rel and RMSELog, respectively. The progress achieved by freezing the encoder and dealing with the significant disparity between source and target data clearly demonstrates the effectiveness of our proposed *FUSE* in addressing the scarcity of event depth data and providing robust and accurate depth estimation. Fig. 4 and Fig. 5 present qualitative comparisons with HMNet[9] for the outdoor_day1 and outdoor_night1 scenes, respectively. *FUSE* provides finer and more stable depth predictions. Compared to HMNet, our method demonstrates a superior ability to preserve structural details, delivering more consistent and accurate predictions on both buildings and vegetation.

Analysis on DENSE Dataset: Tab. II presents the quantitative results on the synthetic DENSE dataset [10]. Our method achieves improvements of 24.9% in Abs.Rel and 33.4% in RMSELog over previous approaches. For the average absolute depth error at the truncated distance, our method ranks either the best or the second-best among the evaluated methods. Fig. 6 shows a qualitative comparison under extreme damage to the image modality. Our *FUSE* is still able to provide stable depth estimation even when some regions of the image are completely destroyed.

C. Ablation Studies

We perform ablation experiments using the ViT-Small model as the backbone on the MVSEC dataset, as outlined in Tab.III. In Baseline-1 and Baseline-2, the model is trained

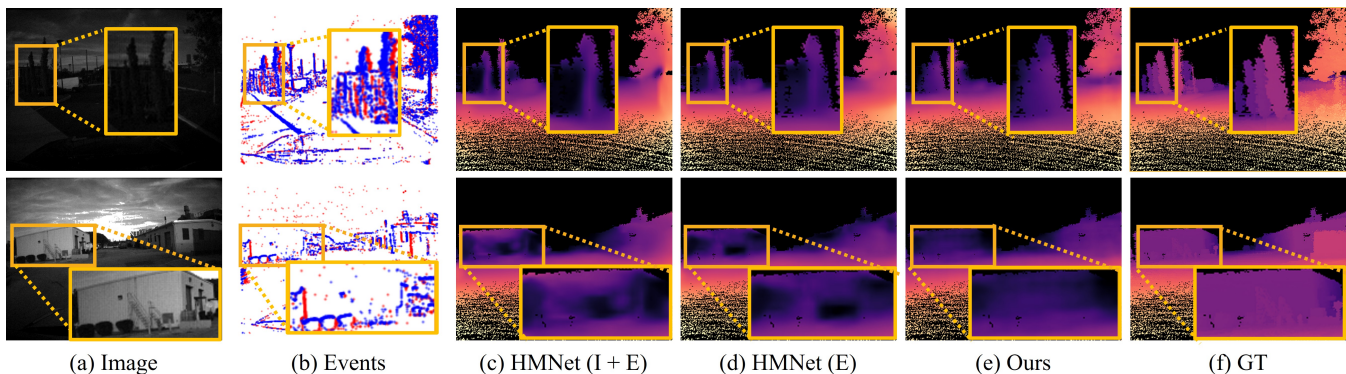


Fig. 4. **Qualitative analysis of the MVSEC dataset, outdoor_day1 scene.** (a) and (b) show the input image and event data; (c) depicts the image-event joint estimation by HMNet[9]; (d) shows the event-only estimation by HMNet; (e) presents our proposed *FUSE*; (f) shows the depth ground truth.

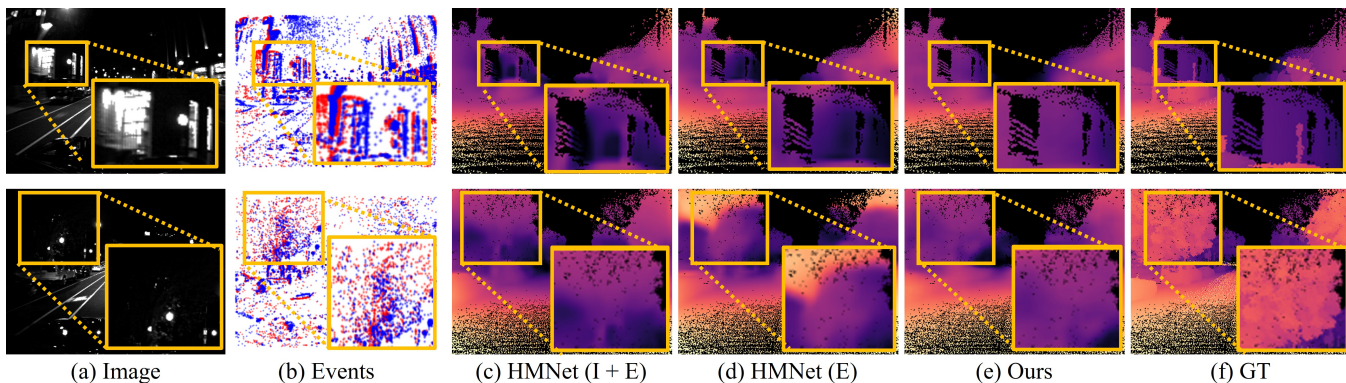


Fig. 5. **Qualitative analysis of the MVSEC dataset, outdoor_night1 scene.** (a) and (b) show the input image and event data; (c) depicts the image-event joint estimation by HMNet[9]; (d) shows the event-only estimation by HMNet; (e) presents our proposed *FUSE*; (f) shows the depth ground truth.

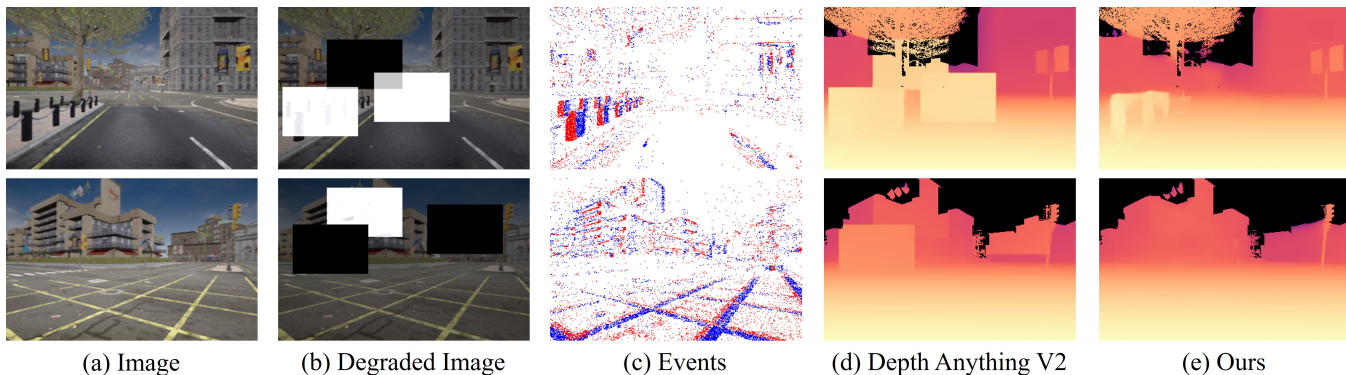


Fig. 6. **Qualitative comparison of zero-shot predictions when the image modality is severely degraded.**(a) denotes the original image, (b) represents the image degraded by low light, overexposure, and occlusion masks, (c) denotes the event data, and (d) and (e) show the predicted results from DepthAnything V2 [28] and our *FUSE*, respectively.

TABLE II
COMPARISON OF PERFORMANCES ON SYNTHETIC DENSE DATASET [10]

Methods	Input	Abs.Rel↓	RMSELog↓	Avg.Error↓		
				10m	20m	30m
RAMNet[6]	I+E	1.189	0.832	2.619	11.264	19.113
SRFNet[17]	I+E	<u>0.513</u>	<u>0.687</u>	<u>1.503</u>	3.566	6.116
<i>FUSE(Ours)</i>	I+E	0.385	0.457	1.286	3.998	6.639

TABLE III
ABLATION STUDIES FOR IMAGE-EVENT FUSION MODELS

	Knowledge Transformer	Feature Fusion Module	Trainable Paras (M)
Baseline-1	None	Cross-Attention	49.2
Baseline-2	None	FredFuse	51.6
Baseline-3	One-stage	FredFuse	6+2.7
<i>FUSE</i>	PST	FredFuse	1.4+4.7+2.7

from scratch on image-event pairs with depth ground truth. Baseline-1 uses two cross-attention mechanisms for feature

fusion, while Baseline-2 incorporates the proposed FredFuse (Sec. III-D). Baseline-3 combines FredFuse with a one-stage knowledge transfer approach, initializing the event encoder with image-based foundation model weights and training

both the event encoder and FreDFuse simultaneously.

Tab. IV and Tab. V present the results of the ablation experiments on the MVSEC dataset, specifically in the outdoor_day1 and outdoor_night1 scenes. The results demonstrate that both components of our proposed method, PST and FreDFuse, positively influence model performance.

Effectiveness of FreDFuse: In the outdoor_day1 scene, Baseline-2 demonstrates an 8% improvement over Baseline-1 in the Abs. Rel metric. Similar improvements are observed across other scenes and metrics. This performance gain can be attributed to FreDFuse’s ability to decouple features into high-frequency and low-frequency branches. By allowing the modality that excels in each branch to dominate the feature fusion, FreDFuse effectively mitigates destructive interference caused by frequency mismatches and enhances inter-modal complementation.

Effectiveness of PST: Compared to Baseline-2, *FUSE* integrates our proposed PST, which reduces the training parameters by 82.2% while achieving an average performance improvement of 19.7% across all metrics and scenarios. This finding suggests that PST can effectively leverage the knowledge from image-based foundation models to mitigate the data scarcity issue in image-event joint depth estimation. In comparison to Baseline-3, *FUSE*, which employs the complete two-stage knowledge transfer process, also shows performance improvements on most metrics in various scenarios. This highlights the significance of the two-stage training with degraded image-event pairs for enhancing the model’s generalization and robustness.

V. CONCLUSION

In this paper, we propose *FUSE*, a novel framework that addresses two fundamental challenges in image-event joint depth estimation: cross-modal knowledge transfer under extreme data scarcity and physics-driven frequency conflicts during feature fusion. By aligning image-event latent spaces through a two-stage adapter tuning strategy, PST successfully transfers geometric priors from image depth foundation models to the joint modality domain without requiring any depth-labeled image-event pairs. This proves that event-depth representations can be effectively bootstrapped from image counterparts when guided by physics-aware constraints, opening new possibilities for data-efficient cross-modal learning. Unlike conventional fusion heuristics, the proposed FreDFuse explicitly resolves the spectral incompatibility between static images (low-frequency dominance) and dynamic events (high-frequency bias) through Gaussian-Laplacian pyramid decomposition. The *FUSE* framework achieves SOTA performance on both real-world (MVSEC) and synthetic (DENSE) benchmarks while enabling lightweight deployment.

While *FUSE* demonstrates strong zero-shot generalization, two limitations warrant further investigation. Current fusion treats events as fixed-interval histograms, potentially underutilizing their microsecond temporal resolution. The framework assumes synchronized image-event pairs, which may not hold for all hardware setups. Future work will

TABLE IV
QUANTITATIVE RESULTS OF THE ABLATION EXPERIMENTS ON THE MVSEC[36] OUTDOOR_DAY1

Methods	$\delta_1 \uparrow$	Abs.Rel \downarrow	RMSE \downarrow	RMSELog \downarrow	Avg.Error \downarrow		
					10m	20m	30m
Baseline-1	0.612	0.366	8.451	0.453	1.711	2.754	3.303
Baseline-2	0.633	0.336	8.403	0.433	1.488	2.519	3.137
Baseline-3	<u>0.704</u>	<u>0.233</u>	<u>6.690</u>	<u>0.313</u>	1.076	1.802	2.210
<i>FUSE</i>	0.719	0.229	6.169	0.294	1.035	1.848	2.267

TABLE V
QUANTITATIVE RESULTS OF THE ABLATION EXPERIMENTS ON THE MVSEC[36] OUTDOOR_NIGHT1

Methods	$\delta_1 \uparrow$	Abs.Rel \downarrow	RMSE \downarrow	RMSELog \downarrow	Avg.Error \downarrow		
					10m	20m	30m
Baseline-1	0.525	0.356	7.698	0.413	1.899	2.634	3.077
Baseline-2	0.531	0.351	7.583	0.418	1.817	2.545	3.018
Baseline-3	<u>0.611</u>	<u>0.268</u>	<u>6.873</u>	<u>0.354</u>	<u>1.326</u>	<u>2.025</u>	<u>2.543</u>
<i>FUSE</i>	0.613	0.267	6.785	0.352	1.305	1.998	2.513

explore event-guided dynamic fusion that adaptively weights frequency branches based on motion intensity, and unsupervised cross-sensor calibration to relax synchronization requirements. These extensions could further solidify image-event depth estimation as a universal solution for extreme environment perception.

REFERENCES

- [1] Shariq Farooq Bhat, Ibraheem Alhashim, and Peter Wonka. “Adabins: Depth estimation using adaptive bins”. In: *Proceedings of the IEEE/CVF conference on computer vision and pattern recognition*. 2021, pp. 4009–4018.
- [2] Linwei Chen et al. “Frequency-aware feature fusion for dense image prediction”. In: *IEEE Transactions on Pattern Analysis and Machine Intelligence* (2024).
- [3] Runze Chen et al. “Structure-Centric Robust Monocular Depth Estimation via Knowledge Distillation”. In: *Proceedings of the Asian Conference on Computer Vision*. 2024, pp. 2970–2987.
- [4] David Eigen, Christian Puhresch, and Rob Fergus. “Depth map prediction from a single image using a multi-scale deep network”. In: *Advances in neural information processing systems* 27 (2014).
- [5] Guillermo Gallego et al. “Event-based vision: A survey”. In: *IEEE transactions on pattern analysis and machine intelligence* 44.1 (2020), pp. 154–180.
- [6] Daniel Gehrig et al. “Combining events and frames using recurrent asynchronous multimodal networks for monocular depth prediction”. In: *IEEE Robotics and Automation Letters* 6.2 (2021), pp. 2822–2829.
- [7] Daniel Gehrig et al. “End-to-end learning of representations for asynchronous event-based data”. In: *Proceedings of the IEEE/CVF International Conference on Computer Vision*. 2019, pp. 5633–5643.
- [8] Andreas Geiger et al. “Vision meets Robotics: The KITTI Dataset”. In: *International Journal of Robotics Research (IJRR)* (2013).

- [9] Ryuhei Hamaguchi et al. “Hierarchical neural memory network for low latency event processing”. In: *Proceedings of the IEEE/CVF Conference on Computer Vision and Pattern Recognition*. 2023, pp. 22867–22876.
- [10] Javier Hidalgo-Carri6, Daniel Gehrig, and Davide Scaramuzza. “Learning monocular dense depth from events”. In: *2020 International Conference on 3D Vision (3DV)*. IEEE. 2020, pp. 534–542.
- [11] Edward J Hu et al. “Lora: Low-rank adaptation of large language models.” In: *ICLR 1.2 (2022)*, p. 3.
- [12] Johannes Kopf, Xuejian Rong, and Jia-Bin Huang. “Robust consistent video depth estimation”. In: *Proceedings of the IEEE/CVF Conference on Computer Vision and Pattern Recognition*. 2021, pp. 1611–1621.
- [13] Zhenyu Li et al. “Binsformer: Revisiting adaptive bins for monocular depth estimation”. In: *IEEE Transactions on Image Processing* (2024).
- [14] Haotian Liu et al. “PCDepth: Pattern-based Complementary Learning for Monocular Depth Estimation by Best of Both Worlds”. In: *2024 IEEE/RSJ International Conference on Intelligent Robots and Systems (IROS)*. IEEE. 2024, pp. 11187–11194.
- [15] Xu Liu et al. “Event-based monocular depth estimation with recurrent transformers”. In: *IEEE Transactions on Circuits and Systems for Video Technology* (2024).
- [16] Michael McCloskey and Neal J Cohen. “Catastrophic interference in connectionist networks: The sequential learning problem”. In: *Psychology of learning and motivation*. Vol. 24. Elsevier, 1989, pp. 109–165.
- [17] Tianbo Pan, Zidong Cao, and Lin Wang. “Srfnet: Monocular depth estimation with fine-grained structure via spatial reliability-oriented fusion of frames and events”. In: *2024 IEEE International Conference on Robotics and Automation (ICRA)*. IEEE. 2024, pp. 10695–10702.
- [18] Ren6 Ranftl, Alexey Bochkovskiy, and Vladlen Koltun. “Vision transformers for dense prediction”. In: *Proceedings of the IEEE/CVF international conference on computer vision*. 2021, pp. 12179–12188.
- [19] Ren6 Ranftl et al. “Towards robust monocular depth estimation: Mixing datasets for zero-shot cross-dataset transfer”. In: *IEEE transactions on pattern analysis and machine intelligence* 44.3 (2020), pp. 1623–1637.
- [20] Alberto Sabater, Luis Montesano, and Ana C Murillo. “Event transformer. a sparse-aware solution for efficient event data processing”. In: *Proceedings of the IEEE/CVF Conference on Computer Vision and Pattern Recognition*. 2022, pp. 2677–2686.
- [21] Shuwei Shao et al. “Iebins: Iterative elastic bins for monocular depth estimation”. In: *Advances in Neural Information Processing Systems* 36 (2023), pp. 53025–53037.
- [22] Shuwei Shao et al. “Nddepth: Normal-distance assisted monocular depth estimation”. In: *Proceedings of the IEEE/CVF International Conference on Computer Vision*. 2023, pp. 7931–7940.
- [23] Dianxi Shi et al. “Improved event-based dense depth estimation via optical flow compensation”. In: *2023 IEEE International Conference on Robotics and Automation (ICRA)*. IEEE. 2023, pp. 4902–4908.
- [24] Peilun Shi et al. “EVEN: An event-based framework for monocular depth estimation at adverse night conditions”. In: *2023 IEEE International Conference on Robotics and Biomimetics (ROBIO)*. IEEE. 2023, pp. 1–7.
- [25] Nathan Silberman et al. “Indoor segmentation and support inference from rgbd images”. In: *Computer Vision–ECCV 2012: 12th European Conference on Computer Vision, Florence, Italy, October 7–13, 2012, Proceedings, Part V 12*. Springer. 2012, pp. 746–760.
- [26] Xiangtong Wang et al. “What makes the unsupervised monocular depth estimation (UMDE) model training better”. In: *Scientific Reports* 12.1 (2022), p. 21999.
- [27] Jialei Xu et al. “Unveiling the depths: A multi-modal fusion framework for challenging scenarios”. In: *arXiv preprint arXiv:2402.11826* (2024).
- [28] Lihe Yang et al. “Depth anything v2”. In: *Advances in Neural Information Processing Systems* 37 (2025), pp. 21875–21911.
- [29] Lihe Yang et al. “Depth anything: Unleashing the power of large-scale unlabeled data”. In: *Proceedings of the IEEE/CVF Conference on Computer Vision and Pattern Recognition*. 2024, pp. 10371–10381.
- [30] Wei Yin et al. “Metric3d: Towards zero-shot metric 3d prediction from a single image”. In: *Proceedings of the IEEE/CVF International Conference on Computer Vision*. 2023, pp. 9043–9053.
- [31] Weihao Yuan et al. “Neural window fully-connected crfs for monocular depth estimation”. In: *Proceedings of the IEEE/CVF conference on computer vision and pattern recognition*. 2022, pp. 3916–3925.
- [32] Jiaming Zhang et al. “CMX: Cross-modal fusion for RGB-X semantic segmentation with transformers”. In: *IEEE Transactions on intelligent transportation systems* 24.12 (2023), pp. 14679–14694.
- [33] Jiqing Zhang et al. “Object tracking by jointly exploiting frame and event domain”. In: *Proceedings of the IEEE/CVF International Conference on Computer Vision*. 2021, pp. 13043–13052.
- [34] Zhuyun Zhou et al. “Rgb-event fusion for moving object detection in autonomous driving”. In: *2023 IEEE International Conference on Robotics and Automation (ICRA)*. IEEE. 2023, pp. 7808–7815.
- [35] Alex Zihao Zhu et al. “EV-FlowNet: Self-supervised optical flow estimation for event-based cameras”. In: *arXiv preprint arXiv:1802.06898* (2018).
- [36] Alex Zihao Zhu et al. “The multivehicle stereo event camera dataset: An event camera dataset for 3D perception”. In: *IEEE Robotics and Automation Letters* 3.3 (2018), pp. 2032–2039.